Selection of a Single Isotope of Multiply Charged Xenon ($^AXe^{z+}$, A=128–136, z=1–6) by Using a Bradbury–Nielsen Ion Gate

Akihiro Kitashoji, Taiki Yoshikawa, Akimasa Fujihara, Takaaki Kamamori, Shigeki Nashima, Tomoyuki Yatsuhashi

WILEY-VCH

Selection of a Single Isotope of Multiply Charged Xenon (^{A}Xe^{z+}, A = 128–136, z = 1–6) by using Bradbury−Nielsen Ion Gate

Akihiro Kitashoji,[†][a] Taiki Yoshikawa,[†][a] Akimasa Fujihara,[b] Takaaki Kamamori,[c] Shigeki Nashima,[c] and Tomoyuki Yatsuhashi*[a]

Abstract: Ion gate equipped in a tandem mass spectrometer is utilized to select a specific precursor ion, and its fragment ions are then assessed for both a structure analysis and an investigation of the chemical reactions. However, the performance of an ion gate has been judged simply by whether or not the target ion was selected. In this study, we designed, manufactured, constructed, and characterized a Bradbury−Nielsen ion gate (BNG). Further, the actual ion selection ability, i.e., the gate function, of the BNG was measured for the isotopes of Xe^{z+} (z = 1–6). The gate function of our BNG was 36.5±0.5 ns in width and 3–13 ns in rise and fall times. Our BNG provides a simple means of satisfying the requirement of selecting multiply charged molecular cations of small organic molecules as well as large molecules such as protein and peptides.

Introduction

The advent of femtosecond lasers opened up a new means of producing multiply charged molecular cations (MMCs) in abundance [1]. Much attention has been directed toward short-lived MMCs, which are highly charged and unstable (repulsive) MMCs. They show prompt dissociation, namely, a Coulomb explosion [2], due to strong Coulomb repulsions between positive charges in MMCs. Molecular structures during a Coulomb explosion have been investigated using various methods such as covariance mapping [3], momentum imaging [4], photoion−photoion−coincidence spectroscopy [5], and simple measurements of kinetic energy releases [6]. In contrast, long-lived MMCs have not been studied well. For dications, lifetimes on the order of milliseconds to seconds were investigated by ion storage ring technology [7,8]. Recently, we reported that quadruply charged four-atomic molecular cations were produced in abundance and were intact enough to be detected after 10 µs from their birth [9]. Several attractive features, such as high electron affinity, high potential energy, high density of electronic states with various spin multiplicities, and charge-dependent chemistry, are expected for such long-

lived MMCs [8,10−15]. However, little is known about the physical and chemical properties of MMCs, although their characteristic features are attractive as novel reactive species from both fundamental and applied scientific perspectives.
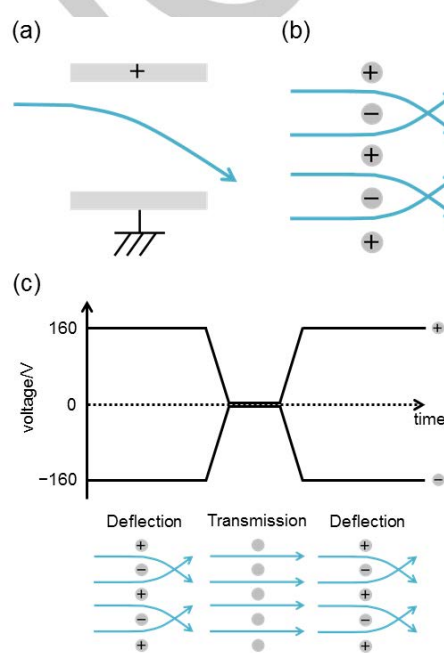
Figure 1. Schematic view of 1) plate electrode-type ion gate, b) Bradbury−Nielsen ion gate (BNG). c) Schematic of BNG operation. Blue arrows indicate ion trajectories.

One subject worth to investigating is the correlation between the chemical reactivity and the charge number of MMCs. The thermal and photochemical reactions of cation radicals have been well explored [16−19]. However, little is known about MMCs except dications [5,20]. Since MMCs are metastable in nature, slow dissociation processes, namely, metastable decays and/or post-source decays (PSDs), are expected to occur when sufficient internal energy is deposited on a precursor MMC. Supposing that we will use time-of-flight mass spectrometry (TOF−MS) for PSD analysis of specific MMCs, the first ion optics (MS1) separate the precursor MMC from the fragment ions formed by prompt dissociations. Then, we need to select an ion packet of a specific precursor MMC (single charge, single isotope) by an ion gate, which alters the flight path of the unwanted ions to the detector. Once the PSD of the selected precursor MMC occurs in the drift (field-free) region of TOF−MS, the resultant fragment (daughter) ions are not accelerated. Therefore, the precursor MMC and its daughter

[a]   Prof. Dr. T. Yatsuhashi, Mr. A. Kitashoji, Mr. T. Yoshikawa
       Graduate School of Science
       Osaka City University
       3−3−138 Sugimoto, Sumiyoshi, Osaka 558−8585 (Japan)
       E-mail: tomo@sci.osaka-cu.ac.jp
       Homepage: http://www.laserchem.jp
[b]   Dr. A. Fujihara
       Graduate School of Science
       Osaka Prefecture University
       1-1 Gakuen-cho, Naka-ku, Sakai, Osaka, Osaka, 599-8531 (Japan)
[c]   Dr. S. Nashima, Mr. T. Kamamori
       Graduate School of Engineering
       Osaka City University
       3−3−138 Sugimoto, Sumiyoshi, Osaka 558−8585 (Japan)
†   These authors contributed equally to this work.

ions have the same velocity and thus the same arrival time to the detector. The ion packet must be further mass-separated by the second ion optics (MS2), namely, the reflectron in order to investigate the distribution of daughter ions. This measurement principle, MS−MS analysis, works well for the investigation of cation radical chemistry [21,22].

However, there are several difficulties in cases of MMCs since the velocity of an MMC depends on the square root of z/m, where z and m denote the charge number and ion mass, respectively. Therefore, the peak separation becomes narrower as z increases and/or m decreases. As a result, we need an ion gate with fast rise and fall times as well as narrow gate width to select an MMC (single charge, single isotope) of small molecules from its adjacent ions. For example, the separation of the quadruply charged 2, 3-benzofluorene ($^{12}C_{17}{}^{1}H_{12}{}^{4+}$, m/z = 54) from its isotope ($^{13}C^{12}C_{16}{}^{1}H_{12}{}^{4+}$, m/z = 54.25) and its hydrogen-loss ion ($^{12}C_{17}{}^{1}H_{11}{}^{4+}$, m/z = 53.75) was 56 ns under our TOF−MS settings [23].

A conventional ion gate consisting of a set of plate electrodes (Fig. 1a) efficiently deflects ion, but the time response is not sufficient for 50-ns gating. In contrast, the Bradbury−Nielsen ion gate (BNG, Fig. 1b) consisting of two interleaved and electronically isolated sets of parallel and equally spaced wires in the same plane, has the potential to deflect ion beams efficiently and quickly by periodically loading transverse electric fields in the adjacent wires [19,22,24−29]. BNG has been widely used in ion mobility spectroscopy experiments, but the gate-width requirement is on the order of several hundreds of microseconds [30,31]. BNG has also been utilized in isobar separation that achieve mass resolution more than 6×10^5 in millisecond flight time [26, 32]. BNG is now being installed in matrix-assisted laser desorption/ionization TOF−MS. However, the performance of a BNG has not been quantitatively evaluated but has been judged simply by whether or not the target ion was selected. It is important to know how quick we can switch the ion trajectories, i.e., diminish (for the ion transmission) and recover (for the ion deflection) electric fields, at an optimal timing to select an MMC (Fig. 1c). In this study, we propose the quantitative evaluation of the total performance of ion gate regardless of the configuration of the gate, a high-voltage power supply, and TOF−MS characteristics.

Results and Discussion

We designed, manufactured, constructed, and characterized a BNG suitable for the study of the MMC chemistry of small organic molecules. A BNG (Figure 2) was constructed as follows: 1) A tungsten wire (10 μm in diameter) was wound around ceramic insulators attached to a square frame (stainless steel, bore size 24×24 mm², thickness 5.0 mm) with 400 μm wire spacing by a home-built wire wounding machine originally designed for manufacturing free-standing wire grids. [33] 2) A pair of metallic plates was fixed on both insulators. Wires were then glued to ceramic insulators. 3) The wires glued between the metallic plates were cut along red broken lines. 4) A pair of wire electrodes was attached each other so that the wires were on

the same plane and spaced 200 μm apart. The slightly disordered wires in the edges of the electrodes were removed so as not to generate inhomogeneous electric fields. There were 74 wires spaced 196.1±15.1 μm (standard deviation was 7.7%) apart, occupying an area of 24.0×14.3 mm². It is noted that the difficulty arising in winding, tensioning and fixing wires can be avoided by using a photo- and/or ion-etched grids as electrodes [25].

BNG was inserted into a vacuum chamber with a z-axis manipulator (ZLTM-114-50HW, VG SCIENTA) so that the BNG was positioned to the optimal ion flight path to the curved-field reflectron and the detector. A high-voltage pulse generator module (HV, PVM-4210, DEI) providing two simultaneous differential voltage pulses was used to apply positive and negative voltages to the adjacent wires of the BNG. The time delay between the synchronization signal of laser and the trigger pulse applied to the HV was controlled by a digital delay/pulse generator (DG645, SRS). The width of the output HV pulse depended on that of the trigger pulse (minimum acceptable trigger pulse width is 50 ns). The shortest output pulse of HV was 42 ns (the full width at half maximum, fwhm) measured by an oscilloscope (TDS-620B, Tektronix) through a high-voltage probe (PPE 1.2 kV, LeCroy). The fall and rise times (10% to 90%) were 8 and 9 ns, respectively.
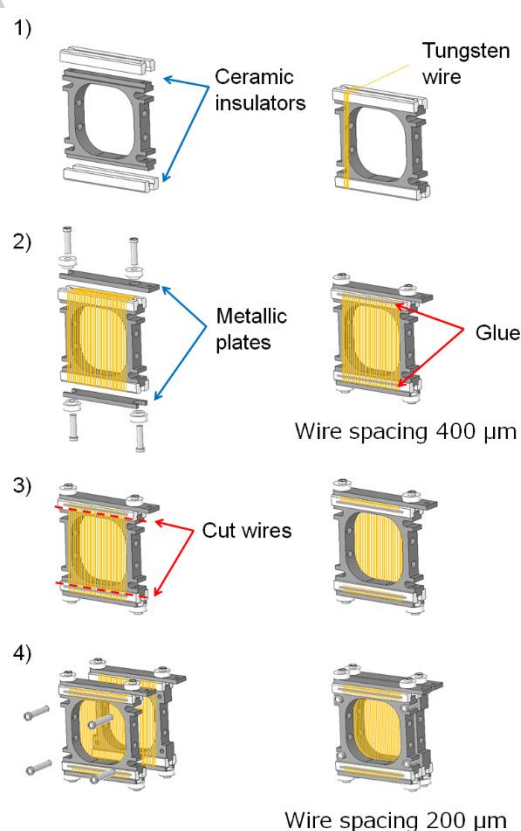
Figure 2. Construction procedure of BNG.

In this study, Xe was exposed to focused femtosecond laser pulses (0.8 μm, linearly polarized, 40 fs, 1 kHz) delivered by a Ti:Sapphire laser (Thales Laser, Alpha 100/1000/XS hybrid). The pressure of Xe was maintained below 5×10^{-5} Pa. Xe was chosen because 1) its mass was on the same order as small organic molecules, 2) its seven isotopes were in similar abundance, and 3) multiply charged cations were formed in abundance. Xe ions were analyzed by a Wiley−McLaren-type TOF−MS equipped with a curved-field reflectron (KNTOF-1800, Toyama) and newly constructed BNG. The output signal from the micro-channel plate (F4655-11X, Hamamatsu Photonics) was averaged by a digital oscilloscope (Wave Runner 6100, 1 GHz, LeCroy) for 1000 shots.

Figure 3a shows the ion yields of Xe as a function of laser intensity. The highest charge number of Xe was 6 at 2.8×10^{15} Wcm^{-2}. As the Xe cations were formed by sequential tunnelling ionization processes [34], the yields of Xe^{z+} (z = 1–5) were saturated at 2.8×10^{15} Wcm^{-2}. The characteristics of multiply charged Xe cation peaks measured at 2.8×10^{15} Wcm^{-2} are summarized in Table 1. The peak separations between adjacent charge numbers were longer than 1 μs. In contrast, the peak separation of two isotopes separated by one mass unit decreased from 129 ns (Xe$^+$) to 52 ns (Xe^{6+}). The peak width (Δt, Gaussian function, fwhm) of a single isotope peak also decreased from 23 ns (^{132}Xe$^+$) to 3.5 ns (^{132}Xe^{6+}). The mass resolution ($m/\Delta m = t/2\Delta t$) was varied from 0.72×10^3 (^{132}Xe$^+$) to 1.9×10^3 (^{132}Xe^{6+}). This variation is due to the saturation effect. The ion peak was sharp below the saturation region of the ion yields [35], and the maximum resolution of ions was ca. 2×10^3. However, the peak became broader in the saturation region due to the spatial distribution of ions. As the laser intensity increases, a higher charge state is formed at the most intense central part of the laser beam, whereas lower charge states are produced at the wing of the laser beam. In this experiment, volume restriction along the laser beam propagation (perpendicular to the ion extraction direction) was successful by the placement of a narrow (500 μm) slit on the extraction electrode. However, the volume along the ion extraction direction could not be restricted [35]. As a result, only the highest charged state, Xe^{6+}, was detected with high resolution at 2.8×10^{15} Wcm^{-2}.
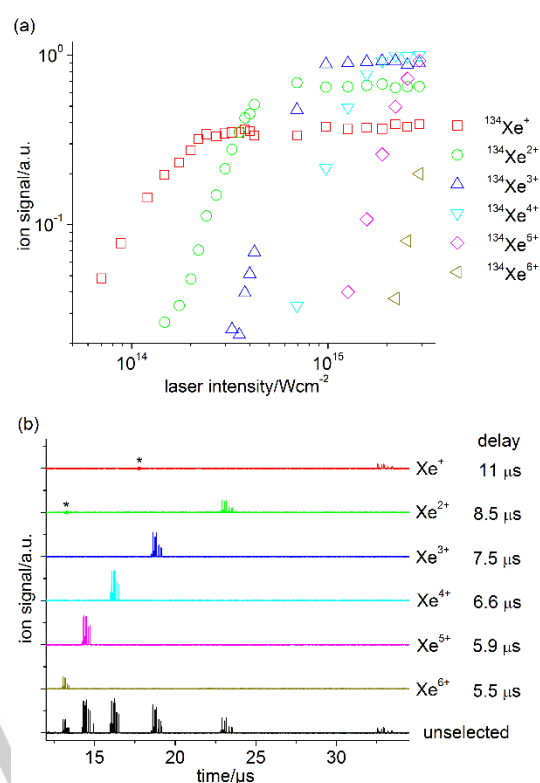
Figure 3. (a) Ion yields of Xe^{z+} as a function of laser intensity. (b) Time-of-flight spectra of a single charge state of Xe^{z+} (z = 1−6) selected by BNG. The right side of each spectrum shows the time delay between the synchronization signal of laser and the trigger pulse applied to a high-voltage pulse generator module for BNG. The bottom shows the unselected spectrum of Xe. The laser intensity was 2.8×10^{15} Wcm^{-2}. * indicates the electrical noise. Detector sensitivity was not corrected.

**Table 1.** The peak separations and peak widths (Δt) of Xe^{z+} (z = 1 − 6)[a]

| z	$t\,(^{132}Xe^{(z-1)+}) - t\,(^{132}Xe^{z+})$[b]	$t\,(^{132}Xe^{z+}) - t\,(^{131}Xe^{z+})$[c]	$\Delta t\,(^{132}Xe^{z+})$[c, d, e]
1	-	129	23 (0.72×10^3)
2	9.8	92	12 (0.94×10^3)
3	4.3	76	9.5 (0.99×10^3)
4	2.6	66	9.0 (0.90×10^3)
5	1.8	59	8.5 (0.84×10^3)
6	1.3	52	3.5 (1.9×10^3)

[a] measured at 2.8×10^{15} Wcm^{-2}. [b] in μs units. [c] in ns units. [d] fwhm. [e] mass resolution ($t/2\Delta t$) is shown in parentheses.

First, seven isotopes of each charge state of Xe^{z+} (z = 1−6) were successfully selected by BNG (Figure 3b) by applying ±160 V (the trigger pulse width was varied between 0.5–7 μs depending on z) to BNG. The total transmittance was 87.3±1.6% (z = 1–6) and was independent of z. The ratio of the peak width (Gaussian function, fwhm) of the selected ion peak to that of an unselected ion peak was 101±1% (z = 1–6) and was independent of z. Thus, it is concluded that BNG did not influence the spatial distribution of the selected ion.

Next, we selected a single isotope peak of Xe^{z+} (z = 1−6) by applying the shortest trigger pulse width (50 ns) to HV. Figure 4 shows the TOF spectra of the individually selected isotopes of $^{A}Xe^{6+}$ (A = 128−132, 134, 136.) and unselected Xe^{6+}. The shape of the selected Xe^{z+} peak except for Xe^{+} was identical to that without applying high voltage to BNG (Figure 5). The shape of the selected Xe^{+} peak was asymmetric and distorted. This is probably because the peak width (23 ns) of Xe^{+} is comparable to that of the gate width. Thus, this distortion would be eliminated simply by enlarging the gate width. The ratio of the peak width (Gaussian function, fwhm) of the selected ion peak to that of the unselected ion peak was 96.4±4.8% (z = 2−6). Though the variation was slightly larger than that measured with a longer gate pulse, it was independent of z. Thus, it is safe to say that the electric field generated in BNG does not interfere with the spatial distribution of the selected ion packet even with the shortest gate width except for Xe^{+}. It should be noted that the total transmittance (131−72%, z = 2−6) was linearly proportional to the reciprocal of the square root of z, hence the flight time. Since the BNG is slightly tilted to the ion flight path and the gate width is close to the peak width, the residual electric field may alter the space-focusing condition and/or the ion flight path. Thus, this mismatch, as clearly seen in the distortion of the selected peak shape of Xe^{+}, might increase or decrease the detection efficiency. In order to achieve uniform ion selection yields, as in the case of a single charge number selection (Figure 3b), the optimization of the gate width, so as not to change the peak shape, is necessary; otherwise, TOF−MS settings such as deflector and reflectron voltages, as well as the tilt angle of the reflectron with respect to the ion flight path, are required.
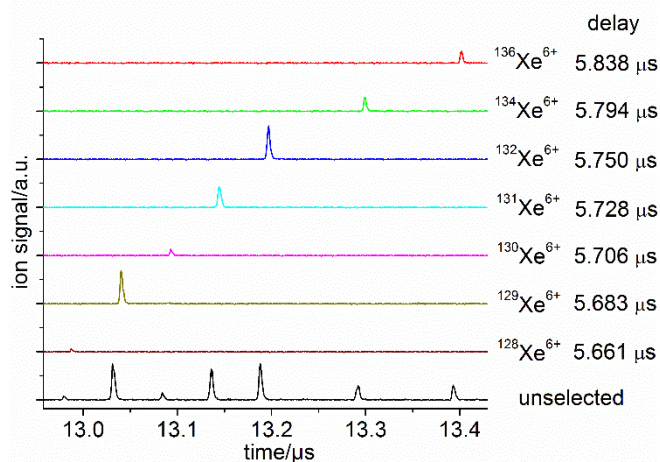
Figure 4. Time-of-flight spectra of a single isotope peak of $^{A}Xe^{6+}$ (A = 128−132, 134, 136). The time delay between the synchronization signal of laser and the trigger pulse applied to the high-voltage pulse generator module for BNG are indicated on the right side of each spectrum. The bottom shows the unselected spectrum of Xe^{6+}. The laser intensity was 2.8×10^{15} Wcm^{-2}.
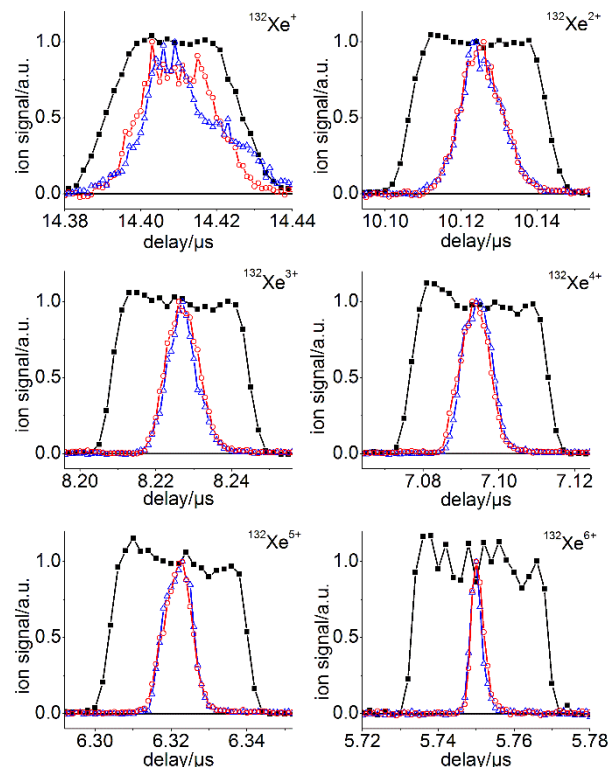
Figure 5. $^{132}Xe^{z+}$ yield (solid square) as a function of the time delay between the synchronization signal of laser and the trigger pulse applied to the high-voltage pulse generator module for BNG. The open triangles and circles, which are plotted on the delay axis, are the corresponding $^{132}Xe^{z+}$ peaks in the time-of-flight spectra with and without high voltage to BNG, respectively. The laser intensity was 2.8×10^{15} Wcm^{-2}.

Finally, we measured the gate function, the ion yields of a single isotope ($^{132}Xe^{z+}$, z = 1−6) as a function of the time-delay between the synchronization signal of laser and the trigger pulse applied to HV (Figure 5). The trigger pulse width was fixed to the minimum value (50 ns). The width (fwhm) of the gate function was 36.5±0.5 ns (z = 1−6), while the rise and fall times (10% to 90%) were dependent on z: 13 ns (Xe^{+}); 7 ns (Xe^{2+}), 6 ns (Xe^{3+}); 5 ns (Xe^{4+} and Xe^{5+}); 3 ns (Xe^{6+}). The shortest rise and fall times were obtained for Xe^{6+}, while the longest ones were obtained for Xe^{+}, since the gate function is the convolution of the actual gate function and the corresponding ion peak.

Conclusions

In conclusion, a BNG capable of selecting a single isotope of multiply charged xenon up to 6+ was successfully constructed and characterized. A method to quantitatively evaluate the actual selection ability, i.e., gate function, of a single ion peak by an ion gate was proposed in this study. The gate function of our BNG was 36.5±0.5 ns (fwhm) in width and 3−13 ns for the rise

and fall times, which were dependent on z. The time separation of the adjacent Xe^{6+} peaks was 52 ns. Since the time separations of the adjacent ions of a quadruply charged organic ion, for example, 2, 3-benzofluorene ($C_{17}H_{12}$) and triphenylene ($C_{18}H_{12}$), were 56 and 58 ns, respectively, under our TOF−MS settings [23], it follows that the performance of our BNG is sufficient to investigate the MMC chemistry of small organic molecules.

The selection ability, i.e., the gate function, depends on the configuration of the BNG and depends strongly on the HV performance. A pair of BNGs, which create the rising and falling edges of the ion packet separately, shortens the gate width [21,28]. This tandem configuration of wire electrodes (50 μmΦ, 0.5 mm spacing) was capable of selecting the ions separated by 56 ns [28]. Although the performance of this tandem BNG has not been quantitatively measured, we emphasize that our single configuration BNG provides a similar level of performance. This is probably due mainly to the performance of HV. In addition, the smaller wire diameter and spacing result in the lower capacitance of BNG, and hence the faster response [27]. Our BNG can be utilized not only to investigate the charge-dependent chemistry of small organic MMCs but also to identify the molecular structures of large molecules such as proteins and peptides.

Acknowledgements

[1]   a) K. W. D. Ledingham, R. P. Singhal, D. J. Smith, T. McCanny, P. Graham, H.S. Kilic, W. X. Peng, S. L. Wang, A. J. Langley, P. F. Taday, C. Kosmidis, *J. Phys. Chem. A* **1998**, *102*, 3002−3005; b) M. Lezius, V. Blanchet, D. M. Rayner, D. M. Villeneuve, A. Stolow, M. Y. Ivanov, *Phys. Rev. Lett.* **2001**, *86*, 51−54; c) M. Murakami, R. Mizoguchi, Y. Shimada, T. Yatsuhashi, N. Nakashima, *Chem. Phys. Lett.* **2005**, *403*, 238−241; d) T. Yatsuhashi, N. Nakashima, *J. Phys. Chem. A* **2005**, *109*, 9414−9418.

[2]   N. Nakashima, S. Shimizu, T. Yatsuhashi, S. Sakabe, and Y. Izawa, *J. Photochem. Phobotiol. C* **2000**, 1, 131−143.

[3]   L. J. Frasinski, K. Codling, P. A. Hatherly, *Science* **1989**, 246, 1029−1031.

[4]   A. Hishikawa, A. Iwamae, K. Yamanouchi, *Phys. Rev. Lett.* **1999**, 83, 1127−1130.

[5]   S. Larimian, S. Erattupuzha, E. Lötstedt, T. Szidarovszky, R. Maurer, S. Roither, M. Schöffler, D. Kartashov, A. Baltuška, K. Yamanouchi, M. Kitzler, X. Xie, *Phys. Rev. A* **2016**, *93*, 053405.

[6]   H. Tanaka, N. Nakashima, T. Yatsuhashi, *J. Phys. Chem. A* **2016**, 120, 6917−6928.

[7]   L. H. Andersen, J. H. Posthumus, O. Vahtras, H. Agren, N. Elander, A. Nunez, A. Scrinzi, M. Natiello, M. Larsson, *Phys. Rev. Lett.* **1993**, 71, 1812−1815.

[8]   D. Mathur, *Phys.Rep.* **2004**, *391*, 1−118.

[9]   T. Yatsuhashi, K. Toyota, N. Mitsubayashi, M. Kozaki, K. Okada, and N. Nakashima, *ChemPhysChem* **2016**, 17, 2977−2981.

[10]   D. Mathur *Phys Rep.* **1993**, 225, 193−272.

[11]   L. Radom, P. M. W. Gill, M. W. Wong, R. H. Nobes, *Pure. Appl. Chem.* **1988**, 60, 183−188.

[12]   D. K. Bohme *Phys. Chem. Chem. Phys.* **2011**, 13, 18253−18263.

[13]   K. Vekey, *Mass Spectrom. Rev.* **1995**, 14, 195−225.

[14]   D. Schröder, *Angew. Chem. Int. Edit.* **2004**, 43, 1329−1331.

[15]   D. Schröder, H. Schwarz, *J. Phys. Chem. A* **1999**, 103, 7385−7394.

[16]   T. Yamazaki, Y. Watanabe, R. Kanya, K. Yamanouchi, *J. Chem. Phys.* **2016**, *144*, 024313.

[17]   R. Itakura, J. Watanabe, A. Hishikawa, K. Yamanouchi, J. Chem. Phys. **2001**, 114, 5598−5606.

[18]   S. P. Ekern, A. G. Marshall, J. Szczepanski, M. Vala, *J. Phys. Chem. A* **1998**, *102*, 3498−3504.

[19]   J. A. Stearns, T. S. Zwier, E. Kraka, D. Cremer, *Phys. Chem. Chem. Phys.* **2006**, *8*, 5317−5327.

[20]   S. D. Price, M. Manning, S. R. Leone, *J. Am. Chem. Soc.* **1994**, 116, 8673−8680.

[21]   C. K. G. Piyadasa, P. Håkansson, T. R. Ariyaratne, D. F. Barofsky, *Rapid. Comm. Mass Spectrom.* **1998**, *12*, 1655−1664.

[22]   R. Weinkauf, K. Walter, C. Weickhardt, U. Boesl, E. W. Schlag, *Z. Naturforsch.* **1989**, *44*, 1219−1225.

[23]   T. Yatsuhashi, N. Nakashima, *J. Phys. Chem. A* **2010**, *114*, 7445−7452.

[24]   N. E. Bradbury, R. A. Nielsen, *Phys. Rev.* **1936**, *49*, 388−393.

[25]   a) T. Brunner, A. R. Mueller, K. O'Sullivan, M. C. Simon, M. Kossick, S. Ettenauer, A. T. Gallant, E. Mané, D. Bishop, M. Good, G. Gratta, J. Dilling, *Int. J. Mass Spectrom.* **2012**, *309*, 97−103, b) I. A. Zuleta, G. K. Barbula, M. D. Robbins, Oh K. Yoon, R. N. Zare, *Anal. Chem.* **2007**, *79*, 9160-9165, c) J. Fox, R. Saini, K. Tsui, G. Verbeck, *Rev. Sci. Instrum.* **2009**, *80*, 093302.

[26]   R. N. Wolf, D. Beck, K. Blaum, Ch. Böhm, Ch. Borgmann, M. Breitenfeldt, F. Herfurth, A. Herlert, M. Kowalska, S. Kreim, D. Lunney, S. Naimi, D. Neidherr, M. Rosenbusch, L. Schweikhard, J. Stanja, F. Wienholtz, K. Zuber, *Nucl. Instrum. Methods Phys. Res., Sect. A*, **2012**, *686*, 82−90.

[27]   Oh K. Yoon, I. A. Zuleta, M. D. Robbins, G. K. Barbula, R. N. Zare, *J. Am. Soc. Mass Spectrom.* **2007**, *18*, 1901−1908.

[28]   C. W. Stoermer, S. Gilb, J. Friedrich, D. Schooss, M. M. Kappes, *Rev. Sci. Instrum.* **1998**, *69*, 1661−1664.

[29]   P. R. Vlasak, D. J. Beussman, M. R. Davenport, C. G. Enke, *Rev. Sci. Instrum.* **1996**, *67*, 68−72.

[30]   J. C. May, J. N. Dodds, R. T. Kurulugama, G. C. Stafford, J. C. Fjeldsted, and J. A. McLean, *Analyst* **2015**, 140, 6824−6833.

[31]   C. Chen, M. Tabrizchi, W. Wang, H. Li, *Anal. Chem.* **2015**, 87, 7925−7930.

[32]   T. Dickel, W. R. Plaß, A. Becker, U. Czok, H. Geissel, E. Haettner, C. Jesch, W. Kinsel, M. Petrick, C. Scheidenberger, A. Simon, M. I. Yavor, *Nucl. Instrum. Methods Phys. Res., Sect. A*, **2015**, *777*, 172−188.

[33]   A. E. Costley, K. H. Hursey, G. F. Neill, J. M. Ward, *J. Opt. Soc. Am.* **1977**, *67*, 979−981.

[34]   S. L. Chin, C. Rolland, P. B. Corkum, P. Kelly, *Phys. Rev. Lett.* **1988**, 61, 153−156.

[35]   a) T. Yatsuhashi, T. Obayashi, M. Tanaka, M. Murakami, N. Nakashima, *J. Phys. Chem. A* **2006**, *110*, 7763−7771, b) N. Mitsubayashi, T. Yatsuhashi, H. Tanaka, S. Furukawa, M. Kozaki, K. Okada, N. Nakashima, *Int. J. Mass Spectrom.* **2016**, *403*, 43−52.

Entry for the Table of Contents (Please choose one layout)

Layout 1:

ARTICLE

Pick up a single isotope: A single isotope of Xe^{6+} was successfully selected by using a time-of-flight mass spectrometer equipped with a curved-field reflectron and the newly constructed Bradbury−Nielsen ion gate (BNG). The actual ion selection ability, i.e., the gate function, by BNG was evaluated to be 36.5±0.5 ns (fwhm) in width, which is sufficient to analyze not only multiply charged small organic molecules but also large molecules such as proteins and peptides.
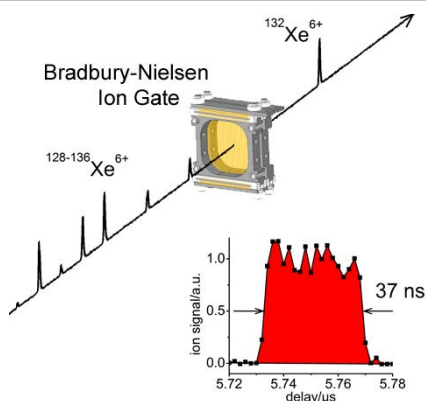
Akihiro Kitashoji, Taiki Yoshikawa, Akimasa Fujihara, Takaaki Kamamori, Shigeki Nashima, and Tomoyuki Yatsuhashi*

Page No. – Page No.

Selection of Single Isotope of Multiply Charged Xenon ($^{A}Xe^{z+}$, A = 128–136, z = 1–6) by using a Bradbury−Nielsen Ion Gate

Layout 2:

ARTICLE

((Insert TOC Graphic here))

Page No. – Page No.